Kinetics and Thermodynamic Parameters of the Thermal Decomposition of Imipramine Hydrochloride and Trimipramine Maleate

RAFIE H. ABU-EITTAH, LAILA T. KAMEL

Department of Chemistry, Faculty of Science, University of Cairo, Giza, Egypt

Received 6 August 2001; accepted 18 October 2002

DOI 10.1002/kin.10107

ABSTRACT: Thermal decomposition of imipramine hydrochloride and trimipramine maleate has been investigated isothermally and nonisothermally. The kinetic parameters, namely the activation energy E_a and the Arrhenius preexponential term A, were calculated. Applying the theory of activated complex to the process of decomposition one calculated $\Delta S^{\neq}$, $\Delta H^{\neq}$, and $\Delta G^{\neq}$ for the reaction. The values of E_a as well as the thermodynamic functions did not vary significantly with temperature of the reaction whereas the preexponential term showed a significant dependence on the reaction temperature. Both imipramine hydrochloride and trimipramine maleate showed two main steps of decomposition. Each step proved to be a first-order reaction. The rate constant was calculated for each step, and the results were analyzed statistically. © 2003 Wiley Periodicals, Inc. Int J Chem Kinet 35: 166–179, 2003

INTRODUCTION

Imipramine hydrochloride and trimipramine maleate are two of the main drugs classified as tricyclic antidepressants [1,2]. These drugs elevate mood, increase physical activity and mental alertness, improve appetite and sleep patterns, and reduce morbid preoccupation in 60–70% of patient with major depression.

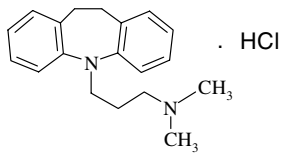

Imipramine Hydrochloride

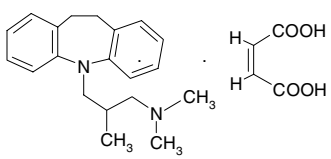

Trimipramine Maleate

Correspondence to: Rafie H. Abu-Eittah; e-mail: rheittah@chem-sci.cairo.eun.eg, abo3ita@hotmail.com.

The osmotic and activity coefficients and excess free energy have been derived as functions of concentration from vapor pressure measurements on aqueous solutions of chlorpromazine, promethazine, and imipramine at 308 and 313 K. The osmotic coefficient is dependent on the concentration and is described by a mass action model of association. A temperature increase increased the critical micelle concentration but had no measurable influence on the aggregation number [3].

The thermal properties of imipramine hydrochloride and trimipramine maleate were studied comparatively by two methods: the TSA (thermomicrotransfer, separation, and the charge treatment) and with a derivatograph [4]. The substances decompose in the 60–100°C range below their melting points. The TSA method was capable of following the decompositions. During studies with the derivatograph, enthalpy changes could not be detected at temperatures below melting ranges of the substances. The compounds are sensitive to oxidizing heat treatment and the fusion products formed are identical to those of thermal decomposition.

Polymorphism of imipramine hydrochloride and other imipramines was studied by thermomicroscopy, thermogravimetry, and differential scanning calorimetry [5]. Heat of fusion and entropy of fusion of imipramine hydrochloride are given. Polymorphism affected the melting points, which are used as criteria of purity of these substances.

The thermal properties of some imipramines including imipramine hydrochloride were studied by differential scanning calorimetry and thermomicroscopy [6]. Melting points, heats of melting, and crystal structure were studied with successive melting and recrystallization. Polymorphism was observed only with some imipramines. Thermomicroscopic data were determined for 44 psychotherapeutic drugs and were tabulated [7].

Thermal analysis is one of the tools that assesses the stability of the compound. It has been recently applied to investigate the decomposition kinetics of Zn(II)–pyrazine polymers [8], where the activation energy E_a of the conversion $[ZnBr_2(pyz)_2]$ to $[ZnBr_2(pyz)]$ is calculated. The aspects and directions of thermal study are many. An important one is thermal study of metal ion complexes of biological importance. The thermal study of theophyllinatoCu(II) complexes of ethanolamine and diethanolamine, a model of metal–guanine interaction, has been investigated [9]. Thermal change takes place in different steps, one of which consists of several slow continous processes and a rapid but overlapping mass loss process.

In this work, the kinetic parameters of activation for decomposition, namely the activation energy E_a and the Arrhenius preexponential factor A, as well as the activation functions $\Delta S^{\neq}$, $\Delta H^{\neq}$, and $\Delta G^{\neq}$, were calculated for imipramine hydrochloride and trimipramine maleate. The results were analyzed statistically. It turned out that E_a, $\Delta H^{\neq}$, and $\Delta G^{\neq}$ are independent of the heating rate. The values of the above functions calculated for an isothermal analysis correlated nicely with those calculated for nonisothermal analysis. On the other hand the parameters A and $\Delta S^{\neq}$ are temperature dependent.

EXPERIMENTAL

Materials

Impramine hydrochloride and trimipramine maleate were supplied by Sigma (St. Louis, MO).

Apparatus

Shimadzu, DTA, and TGA-50 machines were used. The weight of the sample was 10 mg and a platinum cell was used for thermal analysis in nitrogen atmosphere at a rate of flow of 5–20 ml/min.

Mass spectra were run on a GCMS-QP1000EX (Shimadzu) quadropole mass spectrometer. The samples were heated on the direct insert probe for solid materials at a heating rate of 20°C/min, ionization energy of 70 eV, ionization current of 60 mA, and vacuum of 10^{-6} torr.

RESULTS AND DISCUSSION

Imipramine Hydrochloride

Mass Spectrometry. Table I gives the relative intensity of the different fragments in the mass spectrum of imipramine hydrochloride. The most intense peak is due to the fragmentation of N-dimethylamine, the terminal group of the side chain. The results show that the tricyclic system is not broken but is fragmented as one unit.

Nonisothermal Decomposition. Figure 1 shows the TGA and DTG curves for nonisothermal decomposition of imipramine hydrochloride at a heating rate of 5°C/min. The process was repeated at different heating rates, namely 10, 15, 20°C/min and the curves obtained were of the same type as in Fig. 1. In the temperature range $133 < T < 311$°C, the TGA curve

Table I The Relative Intensity of Each Fragment in the Mass Spectrum of Imipramine Hydrochloride

Mass	Intensity	Fragment
36	20.0	HCl
58	100.0	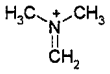
85	54.8	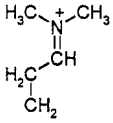
195	22.8	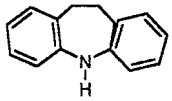
208	20.0	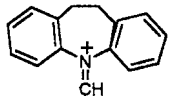
234	56.8	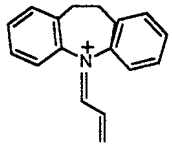
280	20.8	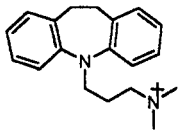

shows an immense decomposition step leading to a weight loss of the order of 70%. The second major step of thermal decomposition is in the temperature range $475 < T < 565$°C. Figure 2 shows the DTA curves for imipramine hydrochloride and trimipramine maleate at a heating rate of 10°C/min under N_2 atmosphere. Two decomposition steps are apparent from the figure. In the light of these results a possible decomposition route of the free base is proposed. In the first step the bond joining the tricyclic ring and the side chain is broken whereas in the second step the side chain is fragmented thus,

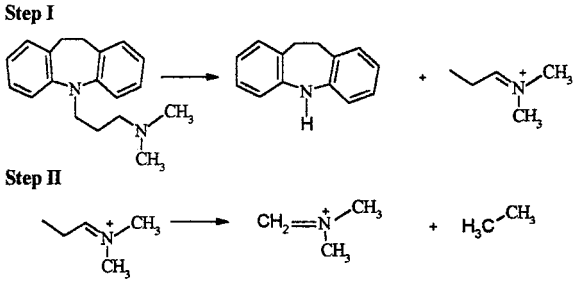

The thermal decomposition of solids is a very complex process. It takes place in several stages as bond breaking; destruction of the initial crystal lattice; formation of the crystal lattice of the solid product;

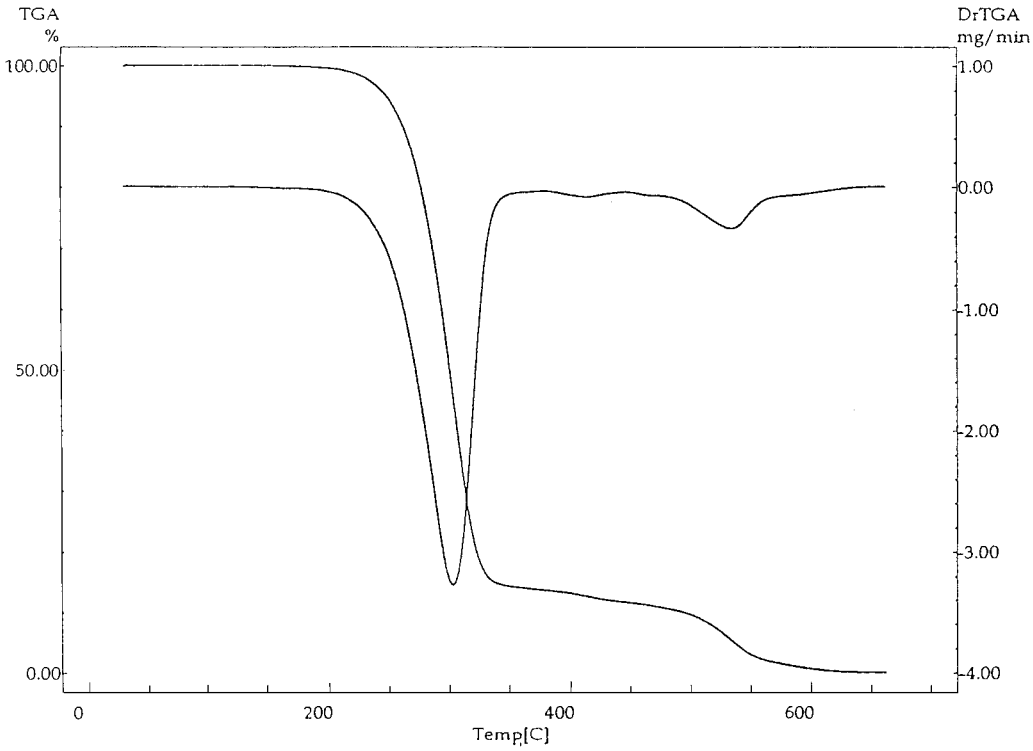

Figure 1 TGA and DTG curves of imipramine hydrochloride at a heating rate of 5°C/min.

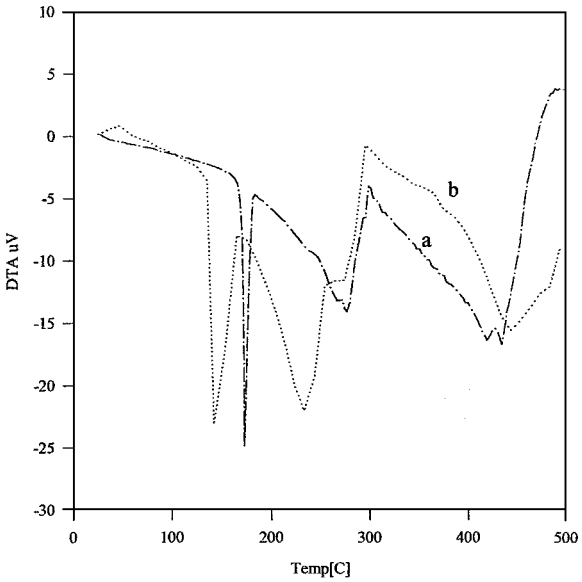

Figure 2 DTA curves of imipramine hydrochloride (a) and trimipramine maleate (b) at a heating rate of 10°C/min.

adsorption–desorption of the gaseous products; and heat transfer. The rate of the thermal decomposition is determined by the rate of one or more of these stages. Other factors, such as particle size, weight of the sample as well as the heating rate, have decisive effect on the rate of pyrolysis. The complexity of the thermal decomposition makes it difficult to find a general equation to describe the kinetics of all the thermal decomposition reactions.

Different computational methods are well established and currently used for investigating the kinetic parameters of thermal decomposition processes. Freeman–Caroll [10], Coats–Redfern [11], Horowitz–Metzger [12], Zsako [13], Satava–Škvarã [14] methods are well established and were used by many authors [15–17].

For solid-state reactions, the rate of a reaction is taken as the change in the fraction reacted, α, with time, i.e. rate $= \mathrm{d}\alpha/\mathrm{d}t$ and is commonly expressed as

$$\text{Rate} = \mathrm{d}\alpha/\mathrm{d}t = k_T f(\alpha) \tag{1}$$

where k_T is the rate constant at temperature T and $f(\alpha)$ is a mathematical function of α [different forms of $f(\alpha)$ has been suggested [10–13]]. In a nonisothermal experiment the temperature of the reaction is controlled to fit a linear programmed rise β(K/min), i.e., $T_t = T_0 + \beta t$. The dependence of the rate constant k_T on the temperature is given by the Arrhenius equation

$$k_T = A\ \exp(-E_\mathrm{a}/RT)$$

The rate equation is then

$$\mathrm{d}\alpha/\mathrm{d}T = A\ \exp(-E_\mathrm{a}/RT) f(\alpha) \tag{2}$$

But

$$\mathrm{d}\alpha/\mathrm{d}t = (\mathrm{d}\alpha/\mathrm{d}T)(\mathrm{d}T/\mathrm{d}t) = (\mathrm{d}\alpha/\mathrm{d}T)\,\beta \tag{3}$$

Combining Eqs. (2) and (3) gives

$$\mathrm{d}\alpha/\mathrm{d}T = \left(\frac{A}{\beta}\right) \exp(-E_\mathrm{a}/RT) f(\alpha) \tag{4}$$

Rearranging and integrating

$$\int \frac{\mathrm{d}\alpha}{f(\alpha)} \equiv g(\alpha) = \left(\frac{A}{\beta}\right) \int \left(\exp\left(-\frac{E_\mathrm{a}}{RT}\right)\right) \mathrm{d}T \tag{5}$$

Two difficulties are encountered: the analytical form of $f(\alpha)$ is generally unknown and the right-hand side of Eq. (5) cannot be integrated in finite form. Coats and Redfern [11] used a general form of Eq. (5) to evaluate the kinetic data from TGA curves as

$$\int_0^\alpha (1-\alpha)^{-n}\,\mathrm{d}\alpha = \left(\frac{A}{\beta}\right) \int_0^T \exp\left(\frac{-E_\mathrm{a}}{RT}\right) \mathrm{d}T \tag{6}$$

where β is the heating rate, T is the absolute temperature at time t, n is the order of the reaction. The nth-order kinetic model has been used as it is the model recommended to evaluate the order of the simple pyrolysis of solids [18,19].

Equation (6) has two solutions, which after taking the logarithm of each side are

For $n = 1$

$$\log\left(\frac{-\log(1-\alpha)}{T^2}\right) = \log\left(\frac{AR}{\beta E_\mathrm{a}}\right)\left(1 - \frac{2RT}{E_\mathrm{a}}\right) - \frac{E_\mathrm{a}}{2.303RT} \tag{7}$$

For $n \neq 1$

$$\log\left(\frac{1-(1-\alpha)^{1-n}}{T^2(1-n^2)}\right) = \log\left(\frac{AR}{\beta E_\mathrm{a}}\right)\left(1 - \frac{2RT}{E_\mathrm{a}}\right) - \frac{E_\mathrm{a}}{2.303RT} \tag{8}$$

For ordinary thermal decomposition reactions, the rate-determining stage at the beginning of the pyrolysis is the same as at the end of the pyrolysis and the process is expressed by the stoichiometric equation

A (s) = B (s) + C (g). The term $\log(AR/\beta E_a)(1 - 2RT/E_a)$ is practically constant and the value of $1 - 2RT/E_a \approx 1$.

Hence

for $n = 1$ a plot of $\log[-\log(1-\alpha)/T^2]$ versus $1/T$ gives a straight line with a slope $-(E_a/2.303R)$ and an intercept $\log(AR/\beta E_a)$.

for $n \neq 1$, a plot of $\log[(1-(1-\alpha)^{1-n})/(T^2(1-n))]$ versus $1/T$ gives a straight line with a slope $-E_a/2.303R$ and an intercept $\log(AR/\beta E_a)$.

Figure 3 shows the variation of α (fraction decomposed) with T, wherein two steps of decomposition are clear. Application of Eqs. (7) and (8) to the decomposition data is shown in Fig. 4, where one gets two segments of straight lines; best straight lines are obtained for $n = 1$ ($Q \equiv$ left-hand side of Eq. (6)). Application of Eq. (6) to each segment is shown in Figs. 5 and 6, whereby distinct straight lines are obtained; the square of the correlation coefficients are 0.998 and 0.978. The fit of Eq. (6) for the first step of decomposition is satisfactory. For step II experimental points appear as if they are sinusoidally distributed along the straight line. This appearance could be a result of the small range of temperature change for step II but the application of Eq. (7) is still valid. The values of the activation energy E_a and the preexponential term A are calculated from the slope and the intercept and are given in Table II.

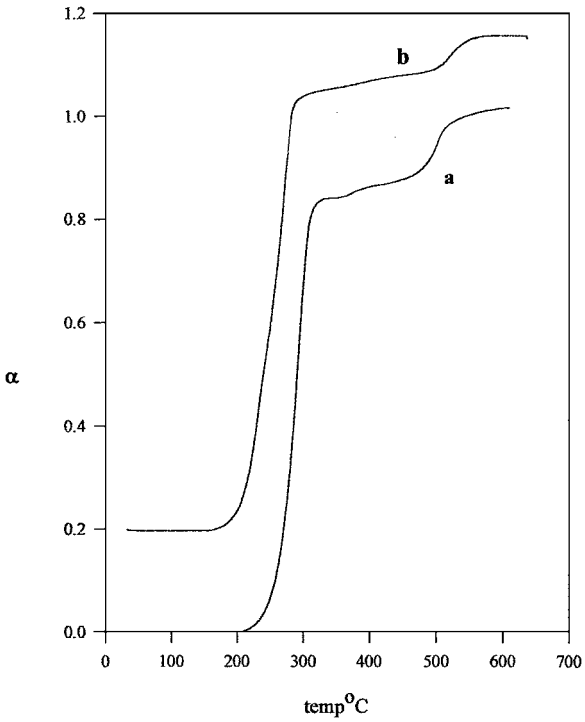

Figure 3 The variation of the fraction decomposed (α) with temperature for imipramine hydrochloride (a) and trimipramine maleate (b).

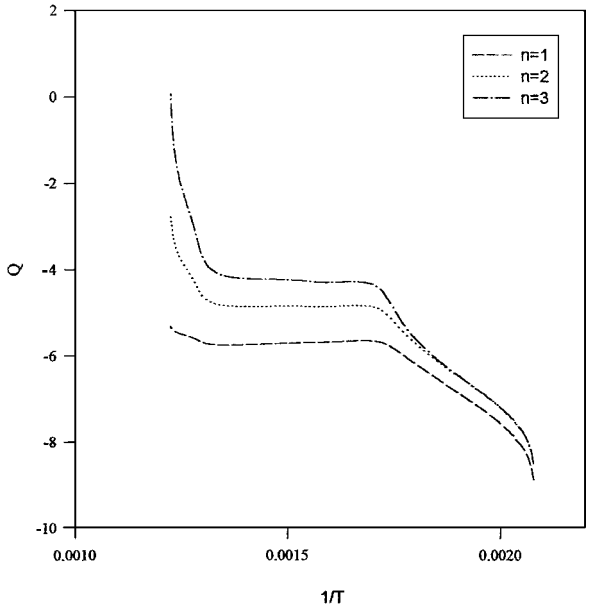

Figure 4 Application of Coats–Redfern relation ($n = 1, 2, 3$) for nonisothermal decomposition of imipramine hydrochloride.

The activated complex theory gives a rate equation, which although simple, provides a framework in terms of which even quite complicated reactions can be understood in a qualitative way, and wherein various assumptions and approximations are involved [20]. The theory has the great advantage of taking into consideration, at least in principle, all the internal motions of the reacting (decomposing) molecule. The potential energy of the molecule, at the time of decomposition, is taken as a function of the relative positions of the various atoms of the molecule. There will be a configuration of atoms of minimum potential energy, related to the activation energy, through which or near which the system (molecule) is expected to pass while going to the products. This region of configuration space is the transition state and the system in the transition state is the activated complex. The transition state theory treats the activated complex formally as a molecule (species) inspite of its ill-defined nature and transitory existence. In this work, the geometry of the decomposing molecule, imipramine or trimipramine bases, is a decisive factor in the rate and mechanism of decomposition. Hence, the application of activation complex theory to the thermal decomposition of the studied molecules is quite adequate.

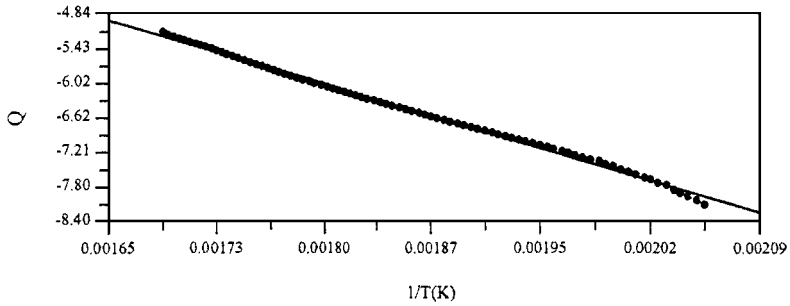

Figure 5 Application of Coats–Redfern relation to the thermal decomposition of imipramine hydrochloride, step I.

The activated complex theory [21] gives the rate constant for a reaction of order n

$$k = \nu^{\neq} K^{\neq} (c^{\circ})^{1-n} \tag{9}$$

where $\nu^{\neq}$ is the decomposition frequency for the activated complex, $K^{\neq}$ is the dimensionless equilibrium constant for the formation of the activated complex, and c° is the standard state concentration. After some mathematical manipulations Eq. (9) becomes

$$k = e^{n} (c^{\circ})^{1-n} \frac{RT}{N_A h} e^{\Delta S^{\neq}/R} e^{-E_a/RT} \tag{10}$$

which leads to a preexponential factor A in the Arrhenius equation as

$$A = e^{n} (c^{\circ})^{1-n} \frac{RT}{N_A h} e^{\Delta S^{\neq}/R} \tag{11}$$

The term c° is the standard state concentration (1 mol/l at pressure of 1 bar and temperature of 298.15 K) and is added in case of bimolecular reactions so as to keep $K^{\neq}$ dimensionless. In case of unimolecular thermal decomposition reactions, c° is unity.

The different terms have their conventional meanings. For $n = 1$ rearrangement of Eq. (11) gives:

$$\Delta S^{\neq} = 2.303 R \log A h / k T_{\mathrm{I}} \tag{12}$$

where k is Boltzmann constant and T_{I} is the peak temperature in the DTG curve. The thermodynamic parameters of activation, formation of active complex just prior to decomposition, were calculated from [18,21]

$$E_a = \Delta H^{\neq} + nRT \tag{13}$$

where n is the order of the reaction. Knowing $\Delta S^{\neq}$, $\Delta H^{\neq}$, and E_a, the values of $\Delta G^{\neq}$, free energy of activation, are calculated. Results are given in Table II.

Some important conclusions are obtained from the results in Table II. The values of E_a and $\Delta G^{\neq}$ did not vary significantly with the heating rate (not significantly dependent on the reaction temperature) whereas the preexponential term A is significantly temperature dependent. The results of this work show that the values of E_a, $\Delta H^{\neq}$, and $\Delta G^{\neq}$ are not the largest for the first step of the thermal reaction inspite of the fact that the largest mass loss is obtained in this step. This result goes along with the fact that the values of E_a, $\Delta H^{\neq}$, and $\Delta G^{\neq}$ depend on the type (strength) of the bond being stretched to arrive at the activated complex (compound just prior to decomposition). The results of this kinetic study indicate that the degrees of freedom of rotation as well as of vibration in the activated compound, a rigid one, are less than they are in the nonactivated compound and this leads to a negative value of $\Delta S^{\neq}$.

Ozawa [22] proposed a method of obtaining the kinetic parameters of a thermal decomposition reaction from TGA curves. He showed that the activation energy can be graphically obtained by following thermogravimetrically the decomposition at different heating rates.

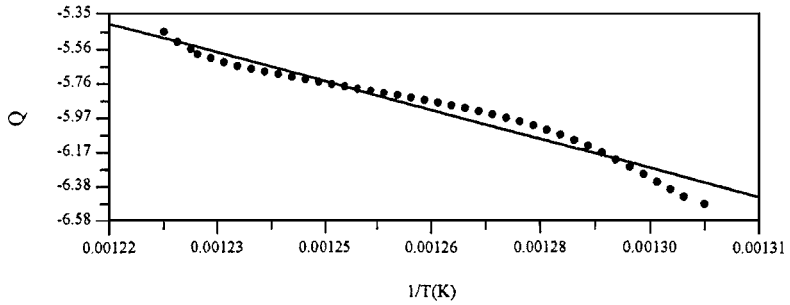

Figure 6 Application of Coats–Redfern relation to the thermal decomposition of imipramine hydrochloride, step II.

Table II Kinetic and Equilibrium Parameters for the Thermal Decomposition of Imipramine Hydrochloride at Different Heating Rates

Step	β (°C/min)	E_a (kJ/mol)	A (s^{-1})	ΔS^* (J/(K mol))	ΔG^* (kJ/mol)	ΔH^* (kJ/mol)
I	5	132	7.90×10^{11}	−22.01	144	128
	10	144	6.90×10^{12}	−4.35	147	140
	15	137	1.16×10^{12}	−19.33	148	132
	20	133	4.88×10^{11}	−26.59	148	202
II	5	194	1.67×10^{11}	−38.25	224	187
	10	205	1.15×10^{13}	−2.73	207	199
	15	208	5.17×10^{12}	−9.75	216	202
	20	194	6.75×10^{11}	−26.50	214	187

The TGA graphs of imipramine hydrochloride at different heating rates are shown in Fig. 7.

According to Ozawa procedures the rate of decomposition is given by

$$-\frac{dW}{dt} = A \exp\left(-\frac{E_a}{RT}\right) W^n \tag{14}$$

where W is the fractional residual weight of the sample, T is the absolute temperature, R is the gas constant, t is the time, A is the preexponential factor, E_a is the activation energy, and n is the order of the reaction.

The fraction weight W of a reacting material is expressed as a function of x, i.e., $W = f(x)$, where x is a structural quantity (such as a group, a constituent, or a broken bond) and changes according to

$$-\frac{dx}{dt} = A \exp\left(-\frac{E_a}{RT}\right) g(x) \tag{15}$$

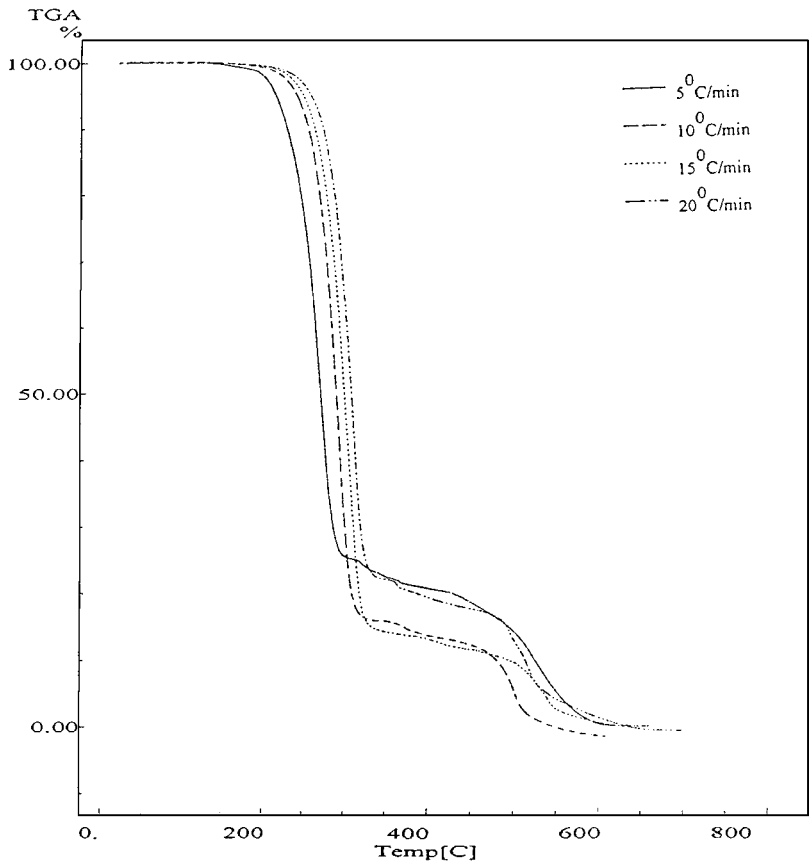

Figure 7 TGA curves of imipramine hydrochloride at different heating rates.

Integration of (15) gives

$$-\int_{x_0}^{x}\frac{dx}{g(x)} = A\int_{t_0}^{t}\exp\left(-\frac{E_a}{RT}\right)dt \qquad (16)$$

If the heating rate β is constant, Eq. (16) becomes

$$-\int_{x_0}^{x}\frac{dx}{g(x)} = \frac{A}{\beta}\int_{T_0}^{T}\exp\left(-\frac{E_a}{RT}\right)dT \qquad (17)$$

where T_0 is the value of T at $t = t_0$.

The rate of the reaction is very low at low temperatures and the following approximation is valid:

$$\int_{T_0}^{T}\exp\left(-\frac{E_a}{RT}\right)dT = \int_{0}^{T}\exp\left(-\frac{E_a}{RT}\right)dT \qquad (18)$$

The right-hand side of (18) is expressed and tabulated by Doyle [23] as the following function of p:

$$\frac{E_a}{R}p\left(\frac{E_a}{RT}\right) = \int_{0}^{T}\exp\left(-\frac{E_a}{RT}\right)dT$$

If the value of E_a/RT is larger than 20, $p(E_a/RT)$ is approximated by

$$\log p\left(\frac{E_a}{RT}\right) = -2.315 - 0.4567\frac{E_a}{RT} \qquad (19)$$

For a given value of W and a single value of x, the left side of Eq. (18) is a constant, which does not depend on the heating rate. Therefore if the weight decreases to a given fraction at the temperature T_1 for the heating rate of β_1, at T_2 for β_2, and so on, the following equations are obtained:

$$\frac{AE_a}{\beta_1 R}p\left(\frac{E_a}{RT_1}\right) = \frac{AE_a}{\beta_2 R}p\left(\frac{E_a}{RT_2}\right) = \cdots \qquad (20)$$

Using Eq. (19), one gets

$$-\log\beta_1 - 0.4567\frac{E_a}{RT_1} = -\log\beta_2 - 0.4567\frac{E_a}{RT_2} = \cdots \qquad (21)$$

Thus, the plots of $\log\beta$ versus the reciprocal of absolute temperature for a given value of W must give a straight line, the slope of which gives the activation energy E_a. Figure 8 shows the relation between $\log\beta$ and $1/T$ at different residual weight percents (58–86 wt%) in the thermal decomposition of imipramine hydrochloride. The values of E_a at each residual weight percent are given in Table III. These values are expected to be more accurate than the average value obtained from Table I in the Coats–Redfern approximation.

Isothermal Decomposition. When pyrolysis takes place under the conditions of TGA, K does not remain constant and depends on temperature. Arrhenius

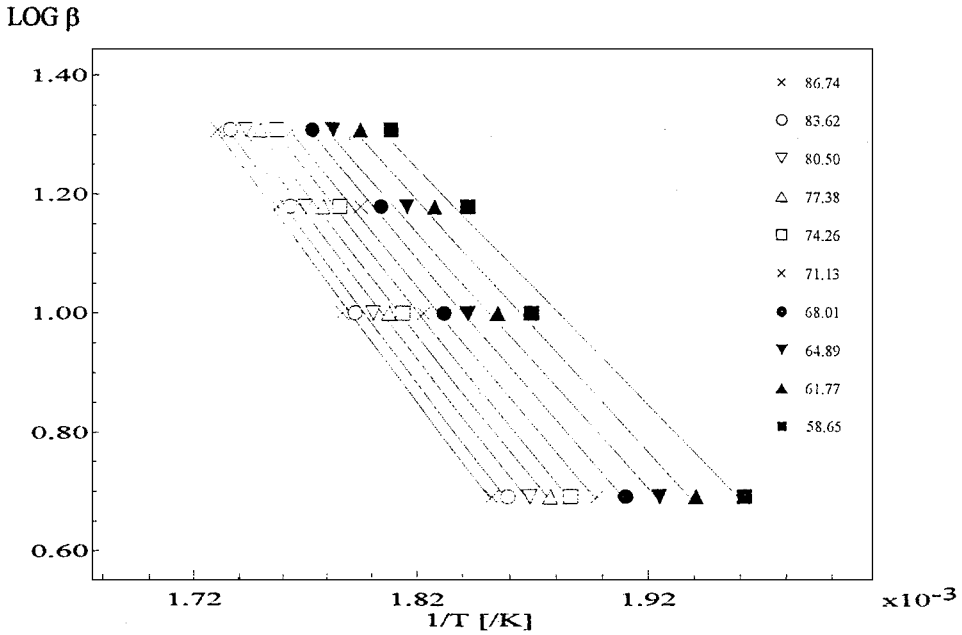

Figure 8 The relation between the logarithm of the heating rate and $1/T$ for different residual weight percents for imipramine hydrochloride.

Table III Activation Energy of the Thermal Decomposition of Imipramine Hydrochloride (A) and Trimipramine Maleate (B) at Different Percents Weight Loss, Step (I)

A		B	
Residual Weight (wt%)	E_a (kJ/mol)	Residual Weight (wt%)	E_a (kJ/mol)
86.74	71.90	90.47	128.72
83.62	75.75	82.03	123.02
80.50	78.36	72.59	123.58
77.38	81.13	65.15	118.10
74.26	83.71	56.70	114.20
71.13	85.63	48.21	111.29
68.01	87.06	39.82	110.42
64.89	88.51	31.38	110.71
61.77	89.89	22.93	110.48
58.65	91.02	14.49	111.30
Average	83.29 ± 6.38		116.19 ± 6.74

relation is persumed for this dependence and it is preferred to treat the process of thermal decomposition isothermally. Ozawa [22] has suggested a method of conversion of the data to apply to conditions of constant temperature changes. According to the Ozawa treatment, the preexponential term is given by

$$A = \beta(E_a/RT^2)\exp^{(E_a/RT)} \tag{22}$$

The reduced time θ is defined as

$$\theta = \int_0^t \exp\left(-\frac{E_a}{RT}\right) \mathrm{d}t$$

which at constant temperature becomes

$$\theta = t\exp\left(-\frac{E_a}{RT}\right) \tag{23}$$

and Eq. (15) becomes

$$G(x) = A\theta \tag{24}$$

This is the rate equation used by Ozawa, where A is the frequency factor, the preexponential term in the Arrhenius equation. The function $G(x)$ is related to the reaction quantity and a plot of $G(x)$ against θ gives a straight line passing through the origin, with a slope equal to A. However, in a TGA curve where the reaction is of the nth order, the fraction weight loss C is equivalent to the reaction percent x. The relations between the fraction weight loss C and $G(x)$ is expressed as follows:

- For nth-order reaction

$$G(x) = \frac{1}{n-1}[(1-C)^{1-n} - 1] \quad C = x \tag{25}$$

- For first-order reaction

$$G(x) = -\log(1-C) \tag{26}$$

Figure 9 shows the relation between $G(x)$ and the reduced time θ. Linear regression is used to draw the best straight line passing through the origin. The slope is 1.98×10^7 min^{-1} and is equal to the preexponential factor A.

Horowitz and Metzger [12] have made an asymptotic expansion of $1/T$ at a conventionally chosen temperature in order to have an integrable form of Eq. (17). They found a linear relation between log of right-hand side of Eq. (17) with temperature and calculated E_a from the slope. This approximation has been criticized [13] based on the fact that a thermal decomposition step takes place frequently over a temperature range of 60–80°C, i.e., the asymptotic approach is not quite justifiable. It has been shown that the slope of the abovementioned plot shows a variation of about 25–30%, which introduces a large error in the activation energy data.

The rate constant (rate factor) is calculated from

$$k = A\exp\left(-\frac{E_a}{RT}\right) \tag{27}$$

Results are given in Table IV.

Figure 10 shows the rate diagram of isothermal decomposition of imipramine hydrochloride at 280, 290, 300, 310, 320, and 326°C. The variation of the reaction percent and time at each specific temperature is given.

Table IV Specific Rate Constant of the Thermal Decomposition of Imipramine Hydrochloride (A) and Trimipramine Maleate (B), Step (I)

A		B	
T (°C)	Rate Constant (10^{-5} min^{-1})	T (°C)	Rate Constant (10^{-8} min^{-1})
280	2.51	160	0.46
290	2.71	190	0.76
300	2.92	220	1.18
310	3.14	250	1.74
320	3.36	280	2.45
326	3.50	300	3.03

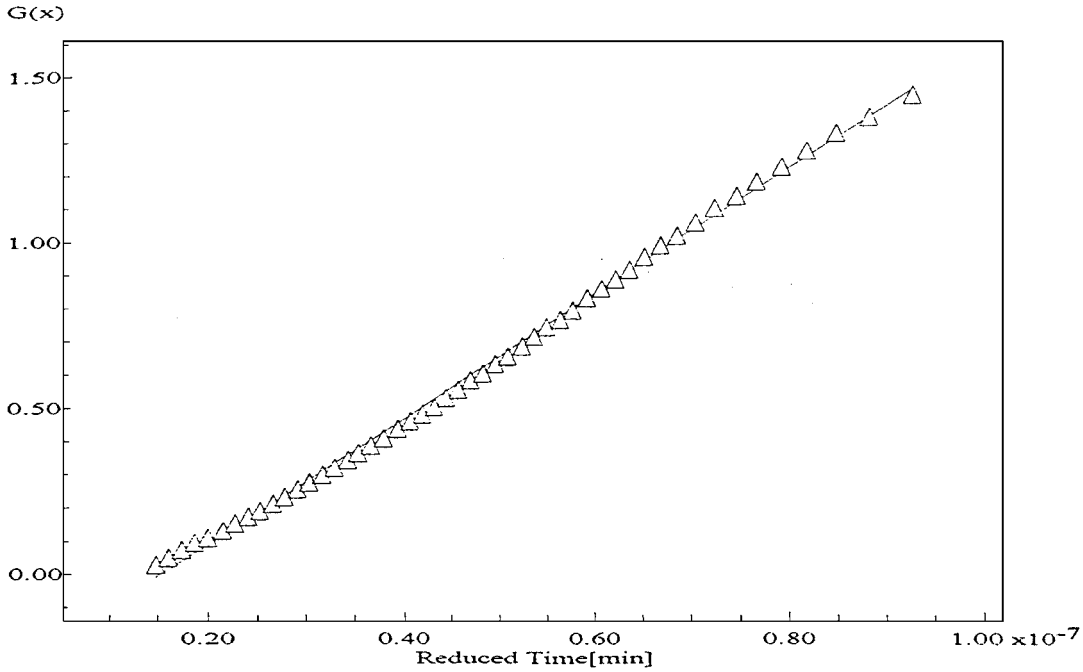

Figure 9 The relation between $G(x)$ and the reduced time θ for imipramine hydrochloride, step I.

Trimipramine Maleate

Mass Spectrometry. Table V shows the relative intensity of each fragment in the mass spectrum of trimipramine maleate. Thermal analysis does not show a number of steps equal to the number of fragments obtained in the mass spectrum. Hence, a stage or a step in the thermal analysis process corresponds to the production of a number of fragments and not just one fragment.

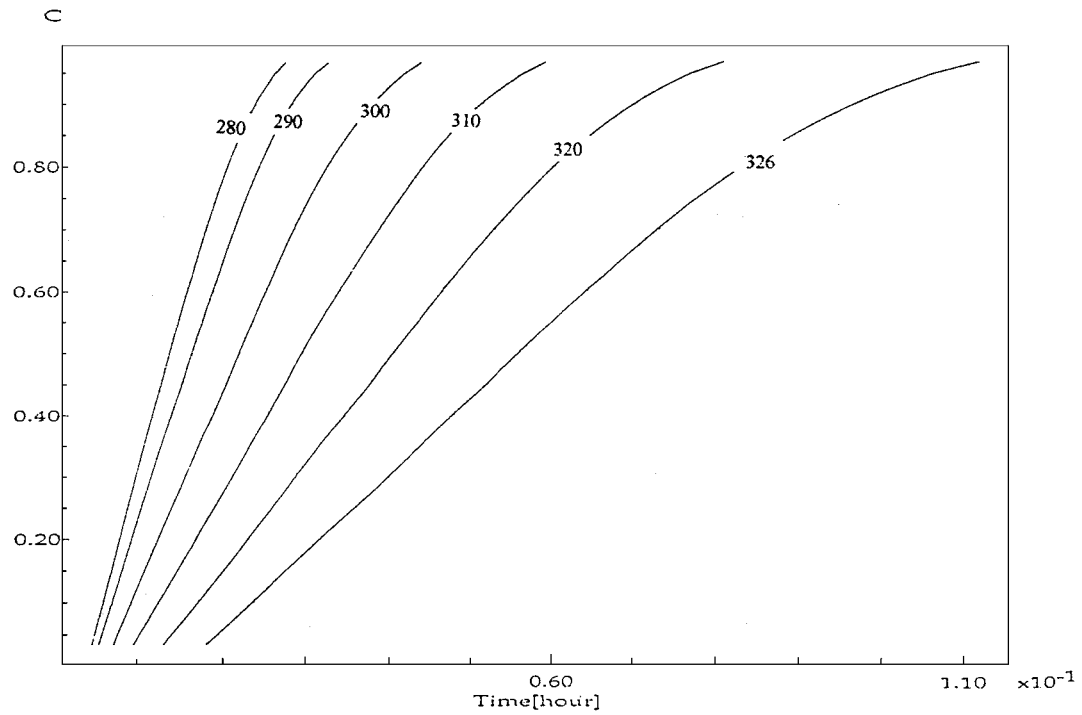

Figure 10 Isothermal decomposition of imipramine hydrochloride at different temperatures, step I.

Table V The Relative Intensity of Each Fragment in the Mass Spectrum of Triimipramine Maleate

Mass	Intensity	Fragment
294	7.6	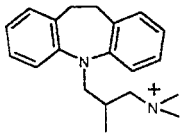
249	48.4	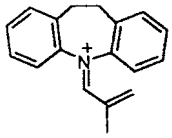
234	8.0	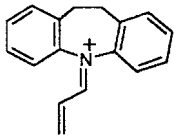
208	22.8	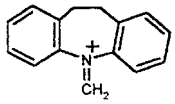
193	14.8	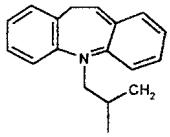
99	17.2	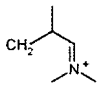
84	10.8	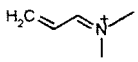
58	100	

Nonisothermal Decomposition. Figure 11 shows the TGA and DTG diagrams of trimipramine maleate at a heating rate of 5°C/min. Similar results were obtained when the heating rates were 10, 15, and 20°C/min. The TGA curve shows two main thermal decomposition steps, but the DTGA curve indicates that the first main step of decomposition (step I) include two substeps. These results are confirmed by studying the DTA of trimipramine maleate, which is shown in Fig. 1. A sharp melting of the compound is observed at 144.8°C.

Figure 3 shows the relation between α (the fraction reacted) and T, where one observes different steps of the reaction. The kinetics of each step of decomposition is investigated separately. Figure 12 shows the relation between Q (where Q is the left-hand side of Eq. (7)) and $1/T$ for the decomposition substep, which is called I_a, that covers the 160–250°C range. The best straight line is obtained for a first-order reaction. On plotting the same relation but assuming other than first-order reactions, straight line relations are not obtained.

Figure 13 shows the relation between Q and $1/T$ for substep I_b in the temperature range 240–300°C. A value of $R^2 = 0.962$ indicating the best straight line relation is obtained, when considering a first-order reaction. The order of the reaction is confirmed by subsequent results. From the slope and intercept of the lines one calculates the activation energy E_a and the preexponential term A. Results are given in Table VI.

The average values of E_a are very comparable for I_a and I_b individual thermal decomposition substeps, a result which indicates the similarity in the type of bonds being broken, extent of fragmentation, and mechanism of the decomposition involved in the two substeps I_a and I_b. The TGA curve shows the clear overlap, continuation, of the two substeps. This is not the case with step II (400–500°C) where one gets much higher values for E_a, almost three times.

Figure 14 shows the relation between Q and $1/T$ for step II of the thermal decomposition of trimipramine maleate. The values of the activation energy E_a and the preexponential term A are given in Table VI. It is seen that the values of E_a are not primarily dependent on the heating rate contrary to the values of A, which are temperature dependent. Both E_a and A are higher for the second step of decomposition than for the first step.

Free activation energy $\Delta G^{\neq}$ (the activated complex is the configuration just before decomposition), activation enthalpy $\Delta H^{\neq}$, and activation entropy $\Delta S^{\neq}$ for the thermal decomposition of trimipramine maleate were calculated and the results are shown in Table VI. The values of these thermodynamic parameters differ significantly for step I than for step II. This indicates that stronger bonds are broken in step II than in step I. A positive value of $\Delta S^{\neq}$ indicates a loosely bound transition state just before decomposition, which leads to a larger number of degrees of freedom for both the rotation and the vibration. On the other hand, a negative $\Delta S^{\neq}$ indicates a rigid activated complex and this leads to a lower number of the degree of freedom for both rotation and vibration.

Isothermal Decomposition. The TGA diagrams for trimipramine maleate at different heating rates were studied. For a specified weight loss the plots between the logarithm of the heating rate and $1/T$ for different residual weight percents (14.49–90.47 wt%) were drawn and nice straight line relations were obtained, a confirmation of a first-order reaction. The slope gives the activation energy E_a. Results are shown in Table III.

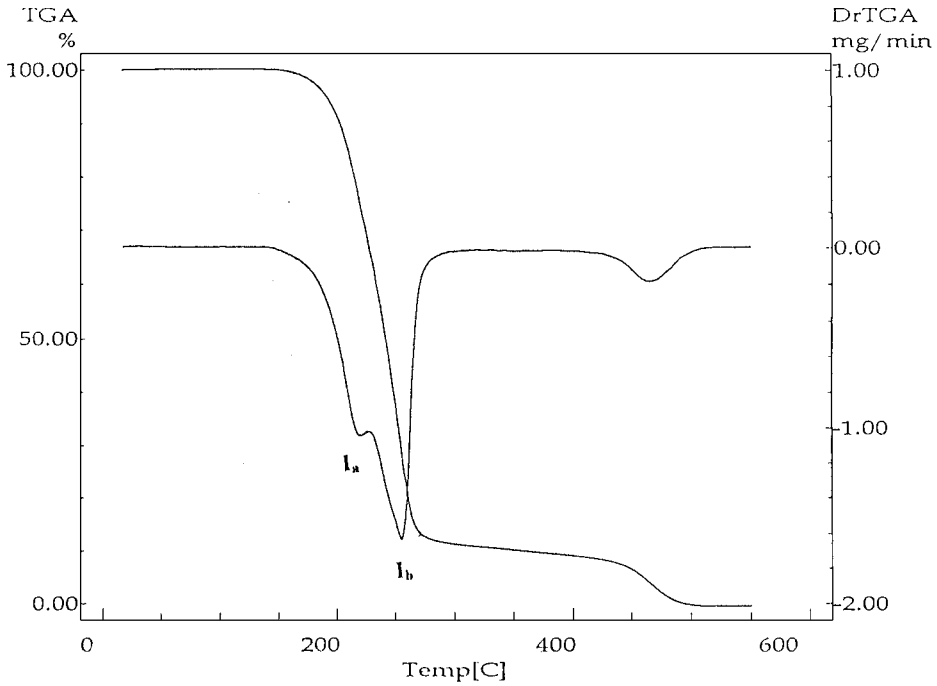

Figure 11 TGA and DTG curves of trimipramine maleate at a heating rate of 5°/min.

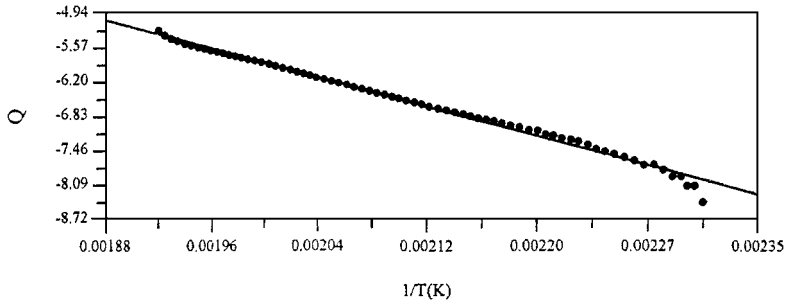

Figure 12 Application of Coats–Redfern relation to the thermal decomposition of trimipramine maleate, step I_a.

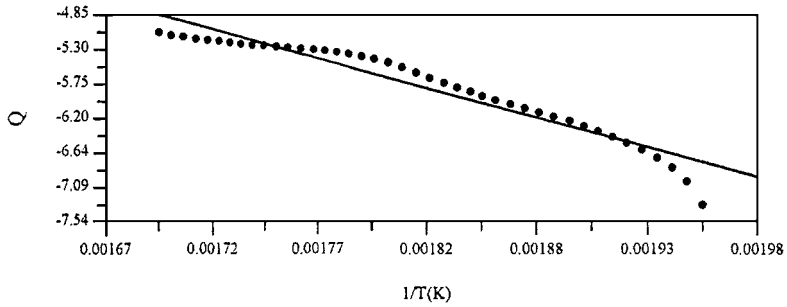

Figure 13 Application of Coats–Redfern relation to the thermal decomposition of trimipramine maleate, step I_b.

Table VI Kinetic Parameters and Thermodynamic Functions of Activation of the Thermal Decomposition of Trimipramine Maleate at Different Heating Rates

Step	β (°C/min)	ΔG^* (kJ/mol)	ΔH^* (kJ/mol)	$-\Delta S^*$ (J/(K mol))	E_a (kJ/mol)	A (s^{-1})
I_a	5	133.72	119.54	20.81	123.59	8.31×10^{11}
	10	130.96	124.71	4.32	128.81	6.07×10^{12}
	15	129.62	128.53	6.15	132.68	2.17×10^{13}
	20	129.62	129.20	8.25	133.39	2.85×10^{13}
I_b	5	141.03	119.22	33.39	123.57	1.96×10^{11}
	10	140.65	120.18	29.93	124.63	3.05×10^{11}
	15	141.53	120.59	30.38	125.09	2.92×10^{11}
	20	142.63	118.49	35.34	123.09	1.64×10^{11}
II	5	200.61	380.09	−252.49	386.19	2.35×10^{26}
	10	209.79	330.19	−163.66	336.64	5.69×10^{21}
	15	209.57	362.87	−202.12	369.44	5.92×10^{23}
	20	207.02	343.67	−178.06	380.36	3.34×10^{22}

The values of E_a at different percent weight losses are given in Table III and agree quite satisfactory with those obtained by applying Coats–Redfern treatment.

The order of the reaction, $n = 1$, is confirmed by the straight line relations obtained on plotting Log β versus $1/T$. Hence, the extent of the reaction function $G(x)$ is calculated based on a first-order reaction. A plot of $G(x)$ against the reduced time θ gave a good straight line relation and the slope gives $A = 1.02 \times 10^{11}$ min^{-1}. Using the average value of $E_a = 116.00 \pm 6.52$ kJ/mol and the value of $A = 1.02 \times 10^{11}$ min^{-1}, one calculates the extent or percentage of the reaction, C, as a function of time at constant temperature, namely 160, 190, 220, 250, 280, 300°C. The specific rate constants are calculated using the Arrhenius equation. Results are given in Table IV.

Step I of the thermal decomposition of trimipramine maleate was pretreated as to consist of substeps I_a (160–240°C), residual weight percent (66.52–99.29 wt%), and substep I_b (240–300°C), residual weight percent (13.91–65.92 wt%), with Ozawa analysis being applied to each substep. Results are given in Tables VII and VIII.

CONCLUSIONS

Mass spectrometry of the studied compounds leads to a large number of fragments with different intensities. On the other hand, thermal analysis indicates that only two main steps are involved in the thermal decomposition reaction. Hence, each step observed in the thermal decomposition possibly includes a number of fragmentations. The first step results in a large weight loss of the order of 70%, and can be divided into two substeps. The kinetics of isothermal as well as nonisothermal decompositions proved that each of the individual steps is a first-order reaction. The calculated kinetic parameters E_a and A, as well as the thermodynamic functions of activation, $\Delta S^{\neq}$, $\Delta H^{\neq}$, and $\Delta G^{\neq}$, have different values for the different steps of thermal decomposition. Generally, the values of these functions are much lower for step I than the corresponding values for step II. This result indicates that bonds broken in step II are much stronger than in step I.

A comparison of Tables II and VI shows that the numerical values of the activation energy E_a and the free activation energy $\Delta G^{\#}$ are comparable for each

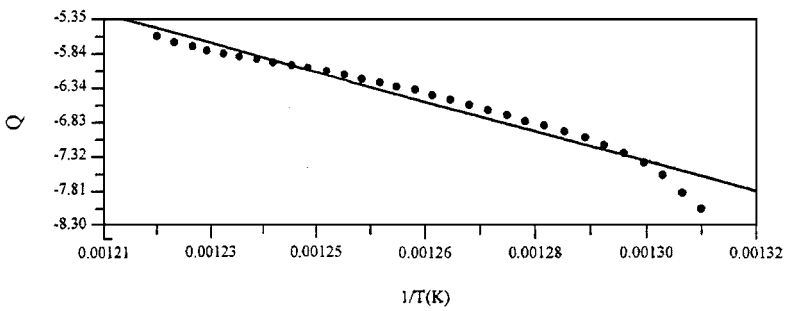

Figure 14 Application of Coats–Redfern relation to the thermal decomposition of trimipramine maleate, step II.

Table VII Activation Energy of the Thermal Decomposition of Trimipramine Maleate for the Two Substeps I_a (160–240°C) and I_b (240–300°C) at Different Percents Weight Loss

Step I_a		Step I_b	
Residual Weight (wt%)	E_a (kJ/mol)	Residual Weight (wt%)	E_a (kJ/mol)
96.29	130.68	65.92	118.39
92.99	128.01	60.15	115.55
89.68	128.11	54.37	113.09
68.37	125.63	48.59	111.09
83.06	123.65	42.01	109.76
79.75	124.18	37.03	111.51
76.45	123.92	31.25	110.86
73.14	123.69	25.47	109.33
69.83	124.60	19.69	107.18
66.52	118.86	13.91	111.85
Average	125.13 ± 3.24		111.82 ± 3.20

step of the thermal decomposition of imipramine hydrochloride and of trimipramine maleate. This is to be expected on the basis of the fact that the main structural unit is the same in the two compounds.

The thermal decomposition of the studied compounds has been carried out at different heating rates. The calculated values of E_a, $\Delta S^{\neq}$, $\Delta H^{\neq}$, and $\Delta G^{\neq}$ showed some dependence on the reaction temperature. This result indicates that the rate-determining process (bond breaking, crystal lattice breaking, etc.) is the same at the beginning and at the end of the specific step of thermal decomposition. Also the kinetics of the reaction (thermal decomposition) does not change through the specific step. In other words the thermal decomposition reaction of the studied compounds is a simple one. On the other hand the Arrhenius preexponential factor A is highly dependent on the reaction temperatures. A positive value of $\Delta S^{\neq}$ is an indication of a loosely bound transition state that leads to a large number of degrees of freedom for both rotation and vibration. On the other hand a negative value of $\Delta S^{\neq}$ is an indication of a stiff transition state that leads to a small number of degrees of freedom for both rotation and vibration.

Table VIII Specific Rate Constant of Thermal Decomposition of Trimipramine Maleate at Different Temperatures for Substeps I_a and I_b

Step I_a		Step I_b	
T (°C)	Rate Constant (10^{-9} min^{-1})	T (°C)	Rate Constant (10^{-9} min^{-1})
160	0.67	250	0.78
180	2.41	260	0.87
190	3.37	270	0.97
220	4.50	290	1.09
230	6.09	280	1.20
240	6.96	300	1.33

BIBLIOGRAPHY

1. Long, J. W. The Essential Guide to Prescription Drugs; Harper & Row: New York, 1980; pp. 43–46, 339–332.
2. Reynolds, J. E. F.; Prasad, A. B. (Eds.). Martindale, the Extra Pharmacopoeia, 28th ed.; The Pharmaceutical Press: London, 1982; pp. 110–121.
3. Attwood, D.; Mosquera, V.; Villar, V. P. J Chem Soc, Faraday Trans 1 1989, 85(9), 3011–3017.
4. Boldvai, J.; Gotz, M.; Posgay-Kovacs, E. J Therm Anal 1983, 27(1), 57–67.
5. Chauvet; Masse, J. Thermochim Acta 1983, 65(2/3), 179–196.
6. Masse, J.; Chauvet, A.; Malaviolle, R.; Sabon, F. Trav Soc Pharm Montpellier 1976, 36(1), 81–90.
7. Kuhnert-Brand-Staetter, M.; Kramar, G.; Lark, P. D. Michrochem J 1972, 17(6), 639–654.
8. Bourne, S. A.; Kelkenny, M.; Nassimbeni, L. R. J Chem Soc, Dalton Trans 2001, 8, 1176–1179.
9. Madarász, J.; Bombicz, P.; Czugler, M.; Pokol, G. Polyhedron 2000, 19(4), 457–463.
10. Freeman, E. S.; Carroll, B. J Phys Chem 1958, 62, 394.
11. Coats, A. W.; Redfern, J. P. Nature 1964, 201, 68.
12. Horowitz, H. H.; Metzger, G. Anal Chem 1963, 35, 1464.
13. Zsako, J. J Phys Chem 1968, 72, 2406.
14. Satava, V.; Škvarã, F. J Am Ceram Soc 1969, 52, 591.
15. Chen, D. T. Y. J Therm Anal 1974, 6, 109.
16. Chen, D. T. Y.; Fong, P. H. J Therm Anal 1975, 8, 295.
17. Fong, P. H.; Chen, D. T. Y. J Therm Anal 1975, 8, 305.
18. Abd El-Wahab, M. M. M. Thermochim Acta 1995, 256, 271–280.
19. Sestak, J.; Berggren, G. Thermochim Acta 1971, 3, 1.
20. (a) Laidler, K. J. Chemical Kinetics, 3rd ed.; Harper and Row: New York, 1987; p. 88; (b) Frost, A. A.; Pearson, R. G. Kinetics and Mechanism, 2nd ed.; Wiley Eastern: New Delhi, 1970.
21. Alberty, R. A. Physical Chemistry; Wiley: New York, 1988.
22. Ozawa, T. Bull Chem Soc Japan 1965, 38, 1881.
23. Doyle, C. D. J App Polym Sci 1962, 6, 639.